Essentiality of conserved amino acid residues in β-lactamase

Chikunova, A.

Chapter 5

Mutations in two highly conserved residues are beneficial for BlaC

Abstract

Conserved residues are often considered essential, thus substitutions in such residues are expected to have negative influence on properties of a protein. However, mutations in a few highly conserved residues of BlaC were shown to have only a limited negative effect on the enzyme. Two mutants, D179N and N245H, displayed increased antibiotic resistance *in vivo* and were investigated further. For BlaC D179N higher survivability can be attributed to a more stable enzyme. The crystal structure reveals subtle structural changes in the Ω-loop as compared to the structure of wild type BlaC. The mutation N245H leads to an increased catalytic activity. Several substitutions of Asn245 give rise to elevated resistance to the β-lactamase inhibitor avibactam, which can be the consequence of the altered binding site. Possible reasons for why these residues are conserved yet not optimal are discussed.

Introduction

Each family of proteins contains a set of highly conserved amino acid residues that are essential for the general function that these proteins exhibit as a group. If a residue is conserved, it is often used as a proxy for its essentiality and therefore, mutations in such a residue are expected to have a negative effect on the function. If the protein has multiple functions, for example, an enzyme that converts several substrates, improvement of one trait is likely correlated with decline of another. However, as discussed in chapter 2, some conserved residues display virtually no change upon mutation and sometimes mutations even benefit the enzyme. Two such residues of BlaC, Asp179 and Asn245 (Ambler numbering[89]), are discussed here. The mutations N245H and D179N exhibited the most interesting results, yielding mostly positive effects and limited negative downsides.

Asp179 is a highly conserved residue (99.8%, Chapter 2), located in the Ω-loop. In BlaC its side chain makes hydrogen bonds to the side chain of the Asp172 and to the backbone Ala164. Recent literature has described substitutions of Asp179 in other β-lactamases. In the β-lactamases TEM, KPC-2 and SHV[232,233,127] a salt bridge interaction is present between Asp179 and Arg164 (Figure 5.1a)[28]. Disruption of this salt bridge was related to increased activity against ceftazidime (Figure 1.3). In BlaC, this salt bridge is absent because the residue at position 164 is an alanine. PER β-lactamases have an asparagine at position 179, but comparison is complicated because the amino acid sequence in general and the conformation of the Ω-loop in particular in PER enzymes differ considerably from other class A β-lactamases (Figure 5.1b). Two other conserved amino acid residues discussed within this chapter are Asp163 and Leu169 (Figure 5.1a).

Asn245 is located in the β-sheet. This residue is 93% conserved in class A β-lactamases (Chapter 2). The side chain of this residue makes two interactions, with the backbone atoms of Ala67 and Phe68 (Figure 5.2). Due to close proximity of the latter residues to Ser70, these interactions are likely to be important for its positioning or orientation, suggesting that Asn245 has a role in fine-tuning the active site structure.

To understand the reason for conservation further, mutants of Asp179 and Asn245 were analysed for their thermal stability and activity against various substrates *in vivo*. The initial focus on D179N and N245H yields more understanding of the good performance of these mutants, as they exhibited increased stability and increased activity, respectively. Additionally, the BlaC variants D179G and N245S were analysed in detail, as they displayed increased ceftazidime and avibactam resistance, respectively.

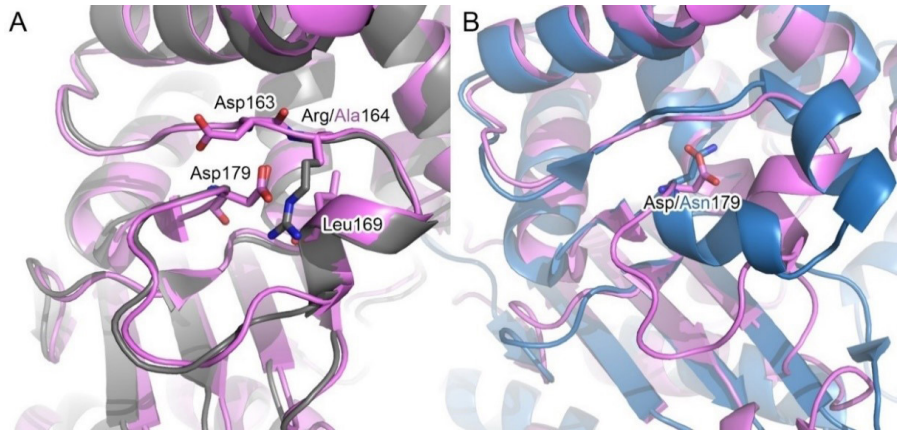

Figure 5.1. Overlay of the structures of BlaC (2GDN[101], in pink) and TEM-1 (1YT4[234], in gray) (A), and PER-2 (4D2O[171], in blue) (B), showing the region around residue 179.

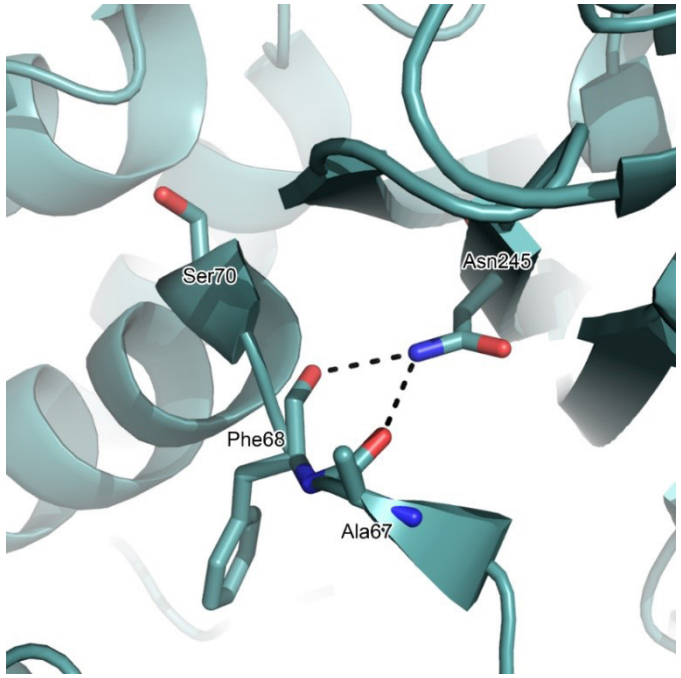

Figure 5.2. Interactions of Asn245 in BlaC (2GDN[101]). Residues Asn245, Ala67, Phe68 and the active site Ser70 are shown in sticks. The dashed lines indicate potential H-bonds.

Results

Activity increase for D179N and N245H is observed in vivo for different classes of β-lactam antibiotics

Mutants D179N and N245H were found to perform better than wild type BlaC *in vivo* against ampicillin and carbenicillin (chapter 2). Often increased activity against one substrate leads to decreased activity against another, therefore *E. coli* cultures producing Asp179 and Asn245 mutants were tested for resistance against other compounds. To determine the minimum inhibitory concentrations (MIC), drops of cell culture diluted 10 - 10,000-fold were applied on agar plates, containing the penicillins ampicillin, carbenicillin or penicillin G, the third-generation cephalosporin ceftazidime or the carbapenem meropenem (Figure 1.3). For evaluation of β-lactamase inhibitor susceptibility, 100 μg mL^{-1} carbenicillin was used in combination with β-lactam β-lactamase inhibitor sulbactam and non-β-lactam β-lactamase inhibitor avibactam.

The results indicated that almost all tested Asp179 mutants outperformed wild type against ceftazidime. D179G mutant was shown to be the most effective, with more than 6-fold increase in MIC (Figure 5.3a). However, only cells producing BlaC D179N displayed increased survival in presence of other β-lactam antibiotics (Table 5.1). Meropenem is a very poor substrate for BlaC, with the wild type enzyme not outperforming a negative control (BlaC S70A) in our screens, thus even the subtle increase in meropenem degradation for D179N mutant (Figure 5.3b). The moderately higher survivability of BlaC D179N with meropenem was shown in liquid culture as well. Previously it was detected that the increase of antibiotic in liquid cultures causes longer horizontal phase (e.g. Figure S5.1), which can be attributed to a degradation of antibiotic by an active enzyme. BlaC D179N variant exhibits shorter horizontal phase than wild type BlaC in presence of meropenem (Figure 5.3b). BlaC D179N also showed somewhat higher resistance to sulbactam and avibactam, which probably can be attributed to an increased conversion of carbenicillin that was used in combination with inhibitors (Figure 5.3c). The increased ceftazidime resistance observed for almost all mutants is remarkable. TEM and KPC β-lactamases[129,130,138] mutants of Asp179 showed the same effect, however, that was attributed to the mutant's inability to form the salt bridge with Arg164. In BlaC this salt bridge is absent due to a R164A substitution, yet we also observe an increase in ceftazidime hydrolysis activity upon mutation of Asp179. In relation to this finding, mutants of two other conserved residues from Ω-loop were analysed for their activity against ampicillin and ceftazidime (Table 5.1) to check if the effect of increased ceftazidime activity is specific to substitutions in Asp179. Mutants of Asp163 (75% conservation) exhibited lost ampicillin activity together with maintained ceftazidime activity at wild type level and most mutants of Leu169 (95% conservation) displayed a loss in ampicillin activity coupled with increased ceftazidime activity (Figure S5.2). These results indicated that the effect of increased ceftazidime activity can be attributed to many modifications in Ω-loop.

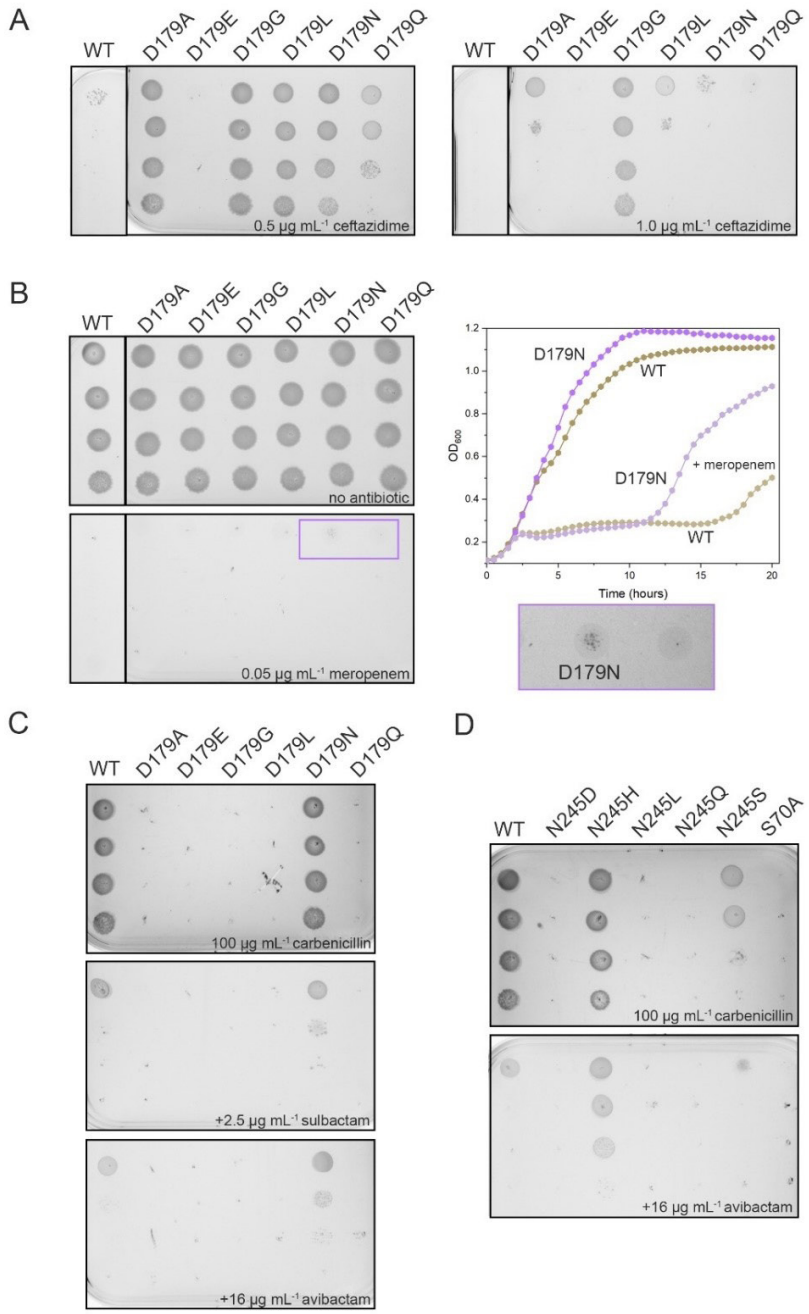

Figure 5.3. (A) Plates and growth curves of BlaC Asp179 variants growing with meropenem. BlaC D179N still exhibits growth on plate with 0.05 µg mL^{-1}meropenem. On the right growth curves of wild type BlaC and BlaC D179N are presented without meropenem and with 0.1 µg mL^{-1}meropenem; (B) Almost all Asp179 variants have higher survivability with ceftazidime than wild type BlaC; (A)-(B) Wild type BlaC panels are from the same LB-agar plates as BlaC variants; (C)-(D) Plates showing growth of Asp179 (C) and Asn245 (D) variants with inhibitors.

Mutations in Asn245 lead to poor ampicillin and ceftazidime degradation for all mutants except for BlaC N245H. Carbenicillin and penicillin G activity suffered to a various degree in Asn245 mutants, however, for BlaC N245H a slightly increased MIC was observed for these substrates as well (Table 5.1). The avibactam and sulbactam inhibition of BlaC N245H was comparable to wild type. For BlaC N245S, sulbactam inhibited growth at 2.5 µg mL^{-1} which is two times lower than for wild type, but N245S also exhibited 2-fold lower MIC against carbenicillin (Table 5.1). With avibactam, however, BlaC N245S was only marginally less sensitive than wild type despite reduced carbenicillin activity (Figure 5.3d). That observation points to a possibly increased avibactam resistance of N245S mutant.

Table 5.1. MIC values of various β-lactams and β-lactamase inhibitors for wild type and mutant BlaC accessed with the droplet test. All MIC values are in µg mL^{-1}. Catalytically inactive BlaC S70A is used as a negative control.

BlaC variant	Ampicillin	Ceftazidime	Meropenem	Carbenicillin	Penicillin G	Avibactam[a]	Sulbactam[a]
WT	80	0.8	0.05	1000	120	>16	5
S70A	20	0.2	0.05[b]	100[b]	40	0	0
D179A	20	**2**	0.05	500	80	0	0
D179E	20	0.2	0.05	500	40	0	0
D179G	20	**5**	0.05	500	40	0	0
D179L	20	**2**	0.05	100	40	0	0
D179N	**120**	**2**	**0.1**	**>1500**	**>120**	**>16**	**7.5**
D179Q	20	**1**	0.05	100	40	0	0
N245D	20	0.2	0.05	100	40	0	0
N245H	80	**2**	0.05	**1500**	**>120**	>16	5
N245L	20	0.2	0.05	100	40	0	0
N245Q	20	0.2	0.05	100	40	0	0
N245S	20	0.2	0.05	500	120	>16	2.5
D163A	20	0.8					
D163E	40	0.8					
D163N	20	0.8					
D163Q	20	0.8					
L199A	20	**1**					
L169E	20	**1**					
L169F	20	**1**					
L169M	40	**1**					
L169V	80	0.8					

[a] Inhibitors were used together with 100 µg ml^{-1} carbenicillin; [b] The minimum concentration tested

Asn245 contributes more to proper folding but less to thermostability than Asp179

The genes of BlaC variants of Asp179 and Asn245 were overexpressed, and the proteins purified. The yield of soluble BlaC D179E, N245D, N245L and N245Q was up to 20 mg of protein from one litre of cell culture. For these mutants, most protein was found in the pellet. Other mutants as well as the wild type BlaC yielded between 40 and 60 mg of soluble protein per litre. BlaC D179N production on the other hand resulted in an increased production of soluble protein with a yield of 150 mg per litre of cell culture. Most but not all mutants exhibited the correct proper fold, as judged by CD spectroscopy (Figure 5.4). Mutants with a low yield also gave aberrant CD spectra.

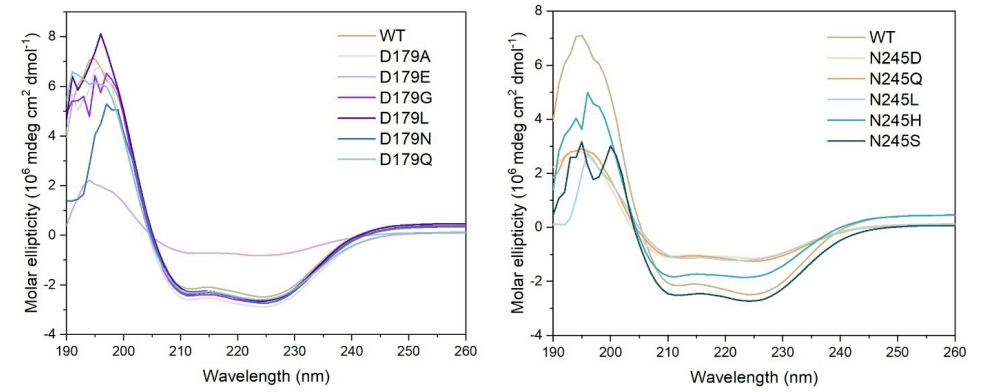

Figure 5.4. CD spectra of BlaC Asp179 and Asn245 mutants.

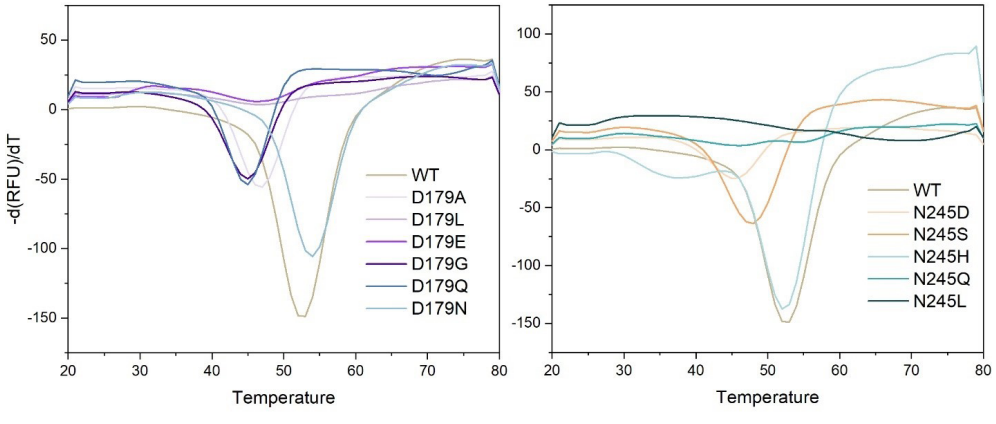

Figure 5.5. Negative derivative of signal from thermal shift assay with the hydrophobic dye SYPRO orange of BlaC Asp179 and Asn245 mutants.

To establish the thermal stability of the BlaC variants, denaturation experiments were performed. Both tryptophan fluorescence and thermal shift assay with hydrophobic dye were used for melting temperature assessment, as these methods might yield structure specific results. The melting temperature of BlaC N245H is close to that of wild type BlaC (Table 5.2, Figure 5.5), whereas for BlaC N245S the melting temperature is 4-5 degrees lower and poorly folded BlaC N245D, N245L and N245Q showed a very gradual unfolding profile upon thermal denaturation, thus melting temperature could not be determined with certainty.

Mutation of Asp179 influenced thermostability more (Table 5.2, Figure 5.5). Substitution with asparagine resulted in 1.5 ˚C increase in melting temperature, whereas substitutions to glycine, glutamine and alanine significantly lowered melting temperature. Due to sample quality, the melting temperature analysis of D179E and D179L was not possible.

Table 5.2. Differences in melting temperature for BlaC variants compared to wild type BlaC. SD standard deviation of three measurements.

BlaC variant	Δ T_m (tryptophan fluorescence) ± SD	Δ T_m (hydrophobic dye)[a]
D179A	-6.3 ± 0.1	-5
D179G	-10.9 ± 0.4	-7
D179N	1.40 ± 0.05	1.5
D179Q	-15.2 ± 1.1	-7
N245D	-6.6 ± 0.1	-7
N245H	-1.2 ± 0.1	0
N245S	-4.50 ± 0.05	-4

[a] Error 0.7 ˚C

Increased in vivo activity of BlaC D179N and N245H has different origins

The kinetic parameters of nitrocefin hydrolysis of BlaC D179N and N245H (Table 5.3, Figure 5.6a) were measured using purified enzymes. BlaC N245H displayed somewhat increased activity. D179N mutant on the other hand, exhibited nitrocefin activity very close to that of wild type BlaC, therefore we attribute the slight increase in activity against most antibiotics *in vivo* of this variant to an elevated production of more stable protein.

Table 5.3. Michaelis-Menten kinetic parameters for nitrocefin hydrolysis. Reactions were carried out in 100 mM sodium phosphate buffer (pH 6.4) at 25 ˚C. Standard deviations (SD) are calculated from triplicate measurements.

BlaC variant	K_M ± SD (μM)	k_{cat} ± SD (s^{-1})	k_{cat}/K_M ± SD ($10^5 M^{-1}s^{-1}$)
WT	263 ± 17	106 ± 5	4.0 ± 0.3
D179N	297 ± 24	98 ± 6	3.3 ± 0.3
N245H	245 ± 8	144 ± 4	5.9 ± 0.2

Asn245 mutants are more avibactam resistant than wild type BlaC

An inhibition assay of nitrocefin hydrolysis using avibactam was performed with wild type enzyme, and BlaC D179N, N245H and N245S. These variants displayed resistance to avibactam *in vivo* at wild type levels or slightly higher. The results indicated that while D179N mutant is inhibited by avibactam similarly to wild type enzyme, both Asn245 mutants are less sensitive to inhibition as they were able to convert relatively more nitrocefin in presence of avibactam (Figure 5.6b). This is clearly visible at 500 μM avibactam at which the mutants N245H and N245S still retain 51% and 47% of initial hydrolysing ability respectively, while for wild type enzyme only 32% of activity is detected. Observation of the nitrocefin hydrolysis over time reveals that the wild type is fully inhibited within 15 min, but N245H and N245S still generate product after 20 min, indicating that full inhibition is not achieved (Figure 5.6c).

Asp179 mutants exhibit changed substrate profile

To address the large increase in ceftazidime MIC coupled with decreased MIC of other compounds for D179G mutant, this variant, together with wild type BlaC and BlaC D179N, were evaluated for their ability to degrade nitrocefin and ceftazidime *in vitro*. The data indicated that BlaC D179G does not display any nitrocefin activity (Figure 5.7a). Ceftazidime degradation with BlaC variants displays two phases (Figure 5.7b). Two-phase ceftazidime hydrolysis was explained before for KPC-2 β-lactamase with the burst phase, caused by rapid acylation and the following linear phase caused by slow deacylation[235]. This explanation does not apply to BlaC, as the amplitude of the burst phase indicates that the enzymes perform more than a single turnover and is substrate concentration dependent. Here, we used the second phase to calculate the "initial" velocities of the reaction (Figure 5.7c). Ceftazidime activity benefits from both the Asp → Asn and Asp → Gly substitution. The catalytic efficiency in the second phase of the reaction for wild type BlaC and BlaC D179N was found to be 46 ± 3 M^{-1} s^{-1} and 160 ± 6 M^{-1} s^{-1} respectively. For BlaC D179G the value could not be calculated with certainty due to the unusual behaviour of this variant with the substrate. It is probable that BlaC D179G exists in two forms with one form responding to a substrate presence slower than the other.

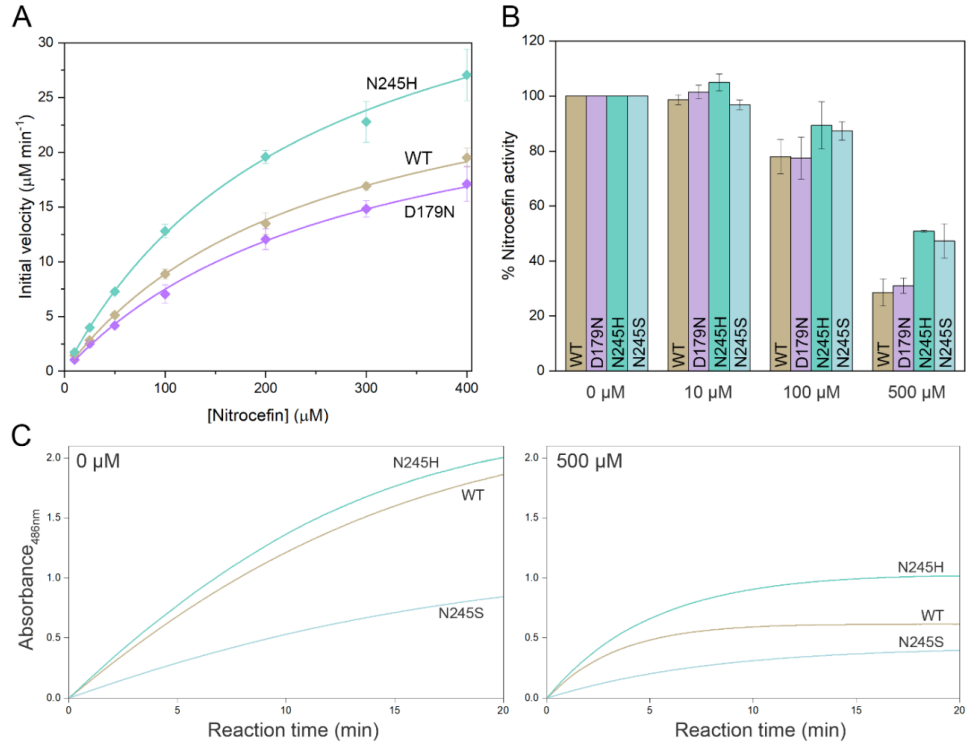

Figure 5.6. (A) Michaelis-Menten curves for reaction with nitrocefin of wild type BlaC, D179N and N245H. Error bars represent standard deviations of triplicates and curves represent the fit to the Michaelis-Menten equation; (B) Relative activity in the absence or presence of avibactam and BlaC measured as amount of hydrolyzed nitrocefin after 20 min at 25 ˚C. Measurements were performed in duplicate in the presence of 100 μM nitrocefin and 2.5 nM BlaC. The error bars represent one standard deviation; (C) Absorbance of the reaction product measured at 486 nm for 20 minutes without avibactam (left) and in presence of 500 μM avibactam (right).

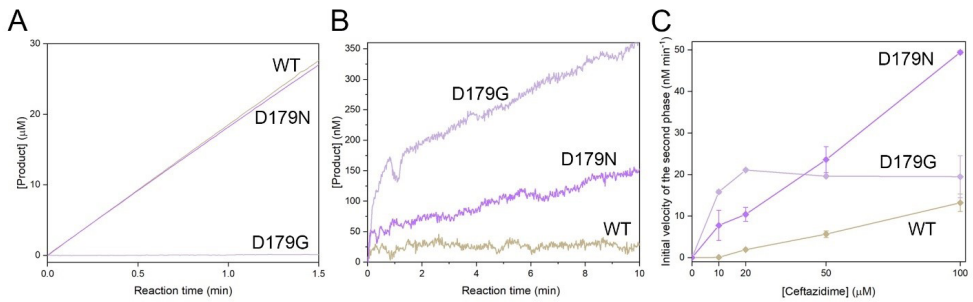

Figure 5.7. (A) Product generation over time in reaction with 400 μM nitrocefin with 5 nM wild type BlaC, BlaC D179N and BlaC D179G; (B) Product generation over time in reaction with 20 μM ceftazidime with 50 nM wild type BlaC, BlaC D179N and BlaC D179G, the burst phase can be observed in the first moments of the reaction followed by the second linear phase; (C) The initial velocity as a function of initial ceftazidime concentration of the second phase kinetics for wild type BlaC and two BlaC Asp179 variants. Error bars represent the standard deviations of duplicate experiments. Data were acquired in 100 mM sodium phosphate buffer (pH 6.4) at 25 ˚C.

Structural changes

^{15}N-^{1}H TROSY-HSQC NMR spectra of BlaC D179N and N245H both indicate the presence of a well-folded enzyme (Figure S5.3). The CSPs of backbone amide resonances for mutant minus wild type are plotted on the crystal structure of wild type BlaC in Figure 5.8a-b. Mutation of Asn245 causes extensive CSPs, covering nearly the whole protein. For BlaC D179N, although changes are also quite spread and involve the active site, the major CSPs are observed for amides in the Ω-loop.

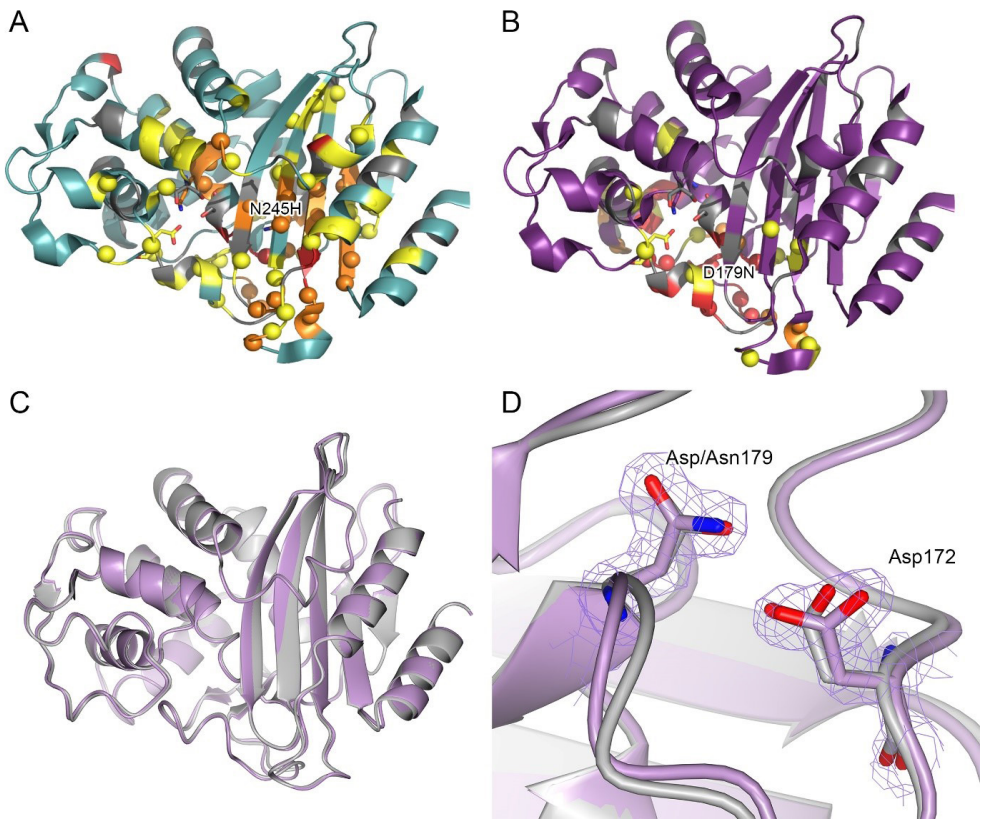

Figure 5.8. (A, B) Average chemical shift differences (CSP) between the resonances of BlaC N245H (A) or BlaC D179N (B) and wild type BlaC mapped on structure (2GDN[101]). Residues are colored yellow for CSP > 0.03 ppm; orange for CSP > 0.05 ppm and red for CSP > 0.1 ppm and gray for no data. The active site residues are shown in sticks; (C-D) Crystal structure of BlaC D179N (lilac) overlaid with wild type structure (2GDN, gray). The 2mF0-DFc electron density map is centered on labeled residues and is shown in purple chicken wire, with contour level 1 σ and extent radius 5 Å.

The crystal structure of the BlaC D179N variant solved at 1.7 Å resolution reveals the nature of the structural changes (Table 5.4, Figure 5.8c-f). Overall, the structure of the mutant resembles the BlaC wild type structure (Cα RMSD 0.31 Å, Figure 5.8c). The newly introduced asparagine occupies the same location as the side chain of aspartate (Figure 5.8d) and the interactions that D179 is involved in are conserved in D179N mutant. In the wild type structure the carboxy-carboxylate interaction requires a shared proton between Asp172 and Asp179[181,182], in BlaC D179N this interaction is an ordinary hydrogen bond between γ-carboxy group of Asp172 and amide group of Asn179. Thus, at near-neutral pH, replacement of one of the carboxy group with a carboxyamide is expected to yield a more stable structure. Noticeable changes concern the Ω-loop of the mutant. Two peptide bonds are flipped in BlaC D179N involving Pro174-Gly175 (Figure 5.9a) and Arg178-Asn179 (Figure 5.9b). The flipped bond involving Arg178 is accompanied by the lost interaction between the side chains of Arg178 and Asp172 and Asp163 and Arg161. Asp163 turns into the solvent and the location previously occupied by its side chain carbonyl is now occupied by the backbone carbonyl of Arg178.

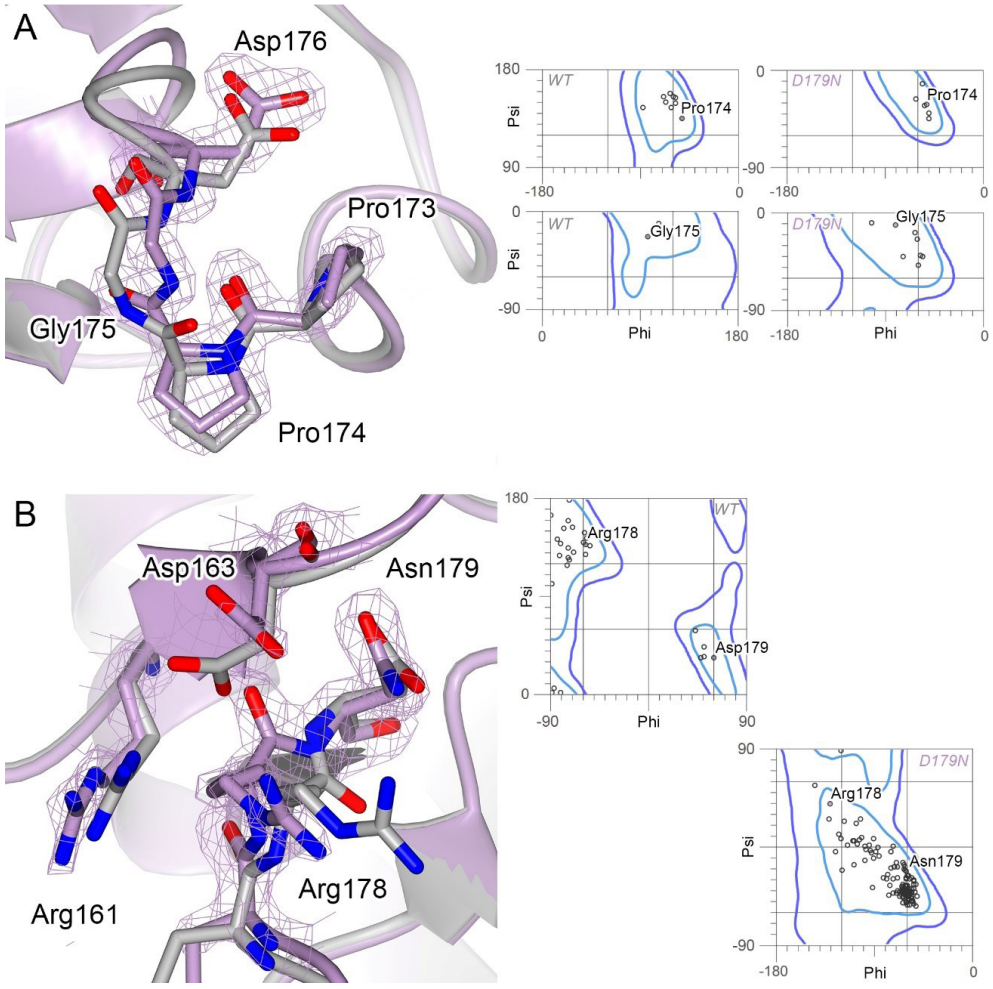

Figure 5.9. Crystal structure of BlaC D179N (lilac) overlaid with wild type structure (2GDN, gray). The 2mF0-DFc electron density map is centered on labeled residues and is shown in purple chicken wire, with contour level 1 σ and extent radius 5 Å. Panels on the right show Ramachandran plots for wild type BlaC and BlaC D179N for the phi-psi of the regions from the left panels.

Discussion

Two residues of BlaC, Asp179 and Asn245, had been identified that are very conserved, yet could be mutated without obvious detrimental effects (chapter 2). For the latter, the initial focus was on mutant N245H because this mutant showed similar or improved resistance traits compared to wild type BlaC. *In vivo* experiments also showed that N245S has increased resistance against avibactam. Also *in vitro* BlaC N245H proved to be more active than wild type and both BlaC N245H and N245S outperformed wild type in an inhibition assay. Asp245 is situated in a β-sheet, in the core of the enzyme, where it makes hydrogen bonds with backbone carbonyl oxygens of Ala67 and Phe68. A mutation from asparagine to histidine fits reasonably well in the stucture of wild type BlaC if it displaces the nearby water molecule (HOH303 in 2GDN). To relieve the remaining steric clashes, slight movement of the β-strands are expected, explaining the extensive CSPs observed around the mutation site. The effects extend into the active site, which could be the cause of the changed activities. The change from Asn to His requires only a single mutation from adenine to cytosine, so it is not obvious why residue 245 is an Asn and not a His in BlaC. It is possible that the Asn is an evolutionary rudiment or the change to His is functionally near neutral.

Asp179 is one of the highly conserved residues of Ω-loop. Within this loop lies the catalytic Glu166 residue, so proper Ω-loop formation is essential for catalysis, although it was shown in Ubbink group and by Nitanai *et al.* that even in deacylation-deficient variants with Glu166 substituted to alanine slow hydrolysis of some cephalosporins can still take place[236]. The most common side chain interactions observed in the Ω-loop of class A β-lactamases are Arg161-Asp163, Glu166-Asn170, and Arg164-Asp179. BlaC does not carry arginine at position 164, thus this salt bridge is missing. The importance of the salt bridge was discussed in multiple studies on various class A β-lactamases. It was shown that mutations in either Arg164 or Asp179 increase resistance against ceftazidime, while decreasing the resistance to other β-lactam antibiotics[130,137,232,235,237,238]. The same effect is observed in our study on BlaC, because almost all mutants of Asp179 showed increased *in vivo* resistance against ceftazidime, with D179G showing the largest increase of 6-fold compared to wild type BlaC, and decreased resistance to other compounds. It can be concluded that, at least in BlaC, the loss of the salt bridge is not the reason for changed substrate profile upon mutation of Asp179 because the salt bridge is not there in the first place. The same effect of increased ceftazidime resistance was also observed for mutants of Asp163 and Leu169 (this study) and a higher ceftazidime MIC was reported for mutant P167S of CTX-M[239]. Another interesting observation is that BlaC D179N exhibits increased MIC values against most tested antibiotics, outperforming wild type BlaC and all other tested mutants, different from what was reported for this mutation in TEM β-lactamase, where increase in ceftazidime MIC comes at a cost of other β-lactam antibiotics activity[129]. However, in KPC-2, the mutation D179N was reported to

improve antibiotic profile, similar to BlaC[240]. This study used modelling to predict the changes in the Ω-loop occurring upon mutation, indicating loss of the Arg164-Asn179 interaction and increased flexibility of Ω-loop. Moreover, molecular modelling revealed changes in the position of catalytic Ser70 and Glu166. An increased flexibility of the Ω-loop is supported by a crystal structure of D179N mutant of PC1 β-lactamase from *Staphylococcus aureus*, where the Ω-loop was found to be disordered[241]. In the crystal structure of BlaC D179N, the loop is highly ordered, however, and only relatively subtle changes are observed. The active site residues do not show any displacement. Two flipped peptide bonds are observed in the Ω-loop of BlaC D179N due to altered interactions between Asp172 and Asn179 and Asp163 and Arg161. The observed changes in the Ω-loop seemingly do not influence the active site or the size of the entrance to the binding site. The NMR data also show few CSPs in the active site, though effects are transmitted to the backside of the protein, probably via Ω-loop residues. It was shown for CTX-M β-lactamase that the mutation P167S causes conformational flexibility in Ω-loop and a large rearrangement of the loop in acyl-enzyme complex[239]. The study showed that in resting state enzyme the loop appeared structurally similar to the wild type protein, however, this mutation allowed the loop to exist in a different conformation with acylated adduct, changing the position of the adduct compared to the adduct in the wild type structure and also influencing the positions of active site residues. This conformational freedom introduced by a mutation can be the reason for its extended substrate profile. The crystal structure or the NMR spectrum of BlaC D179N do not support increased flexibility of the Ω-loop. D179N did not display higher hydrolysing efficiency with nitrocefin, so it is likely that *in vivo* performance of this mutant with antibiotics other than ceftazidime can be attributed mostly to increased stability. However, it remains unclear how the subtle changes observed in the crystal structure can be responsible for an increased ceftazidime activity. The mechanism of conformational change can still be possible in BlaC D179G. Seemingly the Ω-loop of BlaC D179G variant exists in two forms, and the exchange between these forms causes the high amplitude first phase in the ceftazidime kinetics.

The question remains why the effects of the same mutation of an extremely conserved residue differ between β-lactamases. Evolution of β-lactamases even from the same class sometimes takes different pathways. It was demonstrated for TEM and SHV, where substitution R164S in TEM increases ceftazidime activity by almost 100-fold, while in SHV R164S confers only a 2-fold increase[237]. In SHV and TEM, mutation D179G leads to a 5-fold and 7-fold increase in MIC, respectively, so for SHV 179 position substitutions are more beneficial than for TEM. Majiduddin and Palzkill carried out a competition experiment in which D179G mutation outcompeted R164S in SHV, but the contrary happened in TEM. So even though all four mutants provided a better phenotype, in the end only two mutations persisted[237]. Similarly, in clinical isolates substitutions of Asp179 have been observed in SHV[238], but never in TEM. Position 164 is occupied predominantly by arginine in class A β-lactamases, while BlaC carries alanine at this position. The H-bond between Asp172 and Asp179 in BlaC is possible due to the absence of Arg at position 164 as the side chains of Arg164 and Asp172 would clash. This subtle change might be responsible for differences observed upon mutation in Asp179 in different β-lactamases. While D179N in BlaC might aid the stability via improved interaction with Asp172, in other β-lactamases it will likely introduce a negative effect on stability due to the lost salt bridge between Asn179 and Arg164. Asp179 is highly conserved in class A β-lactamases, but so is Arg164, thus it is possible that the absence of arginine allowed BlaC to open a new evolutionary pathway with D179N variant being better, so in that way the wild type, with Asp179, might be considered not fully evolved to it fitness optimum.

Materials and methods

In vivo activity

In vivo experiments were performed with *E. coli* KA797 cells transformed with pUK21 based plasmids. For the on-plate test cells were applied on the agar plates as 10 µL drops with OD_{600} values of 0.3, 0.03, 0.003 and 0.0003. All plates contained 50 µg mL^{-1} kanamycin and 1 mM IPTG. Antibiotics and concentrations used were as follows: 20, 40, 80, 100 and 120 µg mL^{-1} of ampicillin, 100, 500, 1000 and 1500 µg mL^{-1} of carbenicillin, 0.2, 0.5, 0.8, 1, 2 and 5 µg mL^{-1} of ceftazidime, 0.05 and 0.1 µg mL^{-1} of meropenem and 20, 40, 80 and 120 µg mL^{-1} of penicillin G. Avibactam was used in concentrations 4, 8, 12 and 16 µg mL^{-1} and sulbactam was used in concentrations 2.5, 5, 7.5 and 10 µg mL^{-1}, both inhibitors were used in combination with 100 µg mL^{-1} carbenicillin. The MICs were determined as the lowest concentration at which no cell dilution grew. For the soluble culture test cells with the OD_{600} 0.3 were diluted x100 and incubated with at 37 °C overnight with constant shaking. Measurements were performed with Bioscreen C plate reader in duplicate.

Protein production and purification

BlaC was produced using *E. coli* BL21 (DE3) pLysS cells transformed with pET28a plasmids containing the *blaC* gene with an N-terminal His tag and TEV cleavage site. Protein was produced and purified as described in chapter 3.

Circular dichroism spectroscopy

The circular dichroism spectra were acquired in a 1 mm quartz cuvette at 25 °C with a Jasco J-815 spectropolarimeter. Samples contained 100 mM sodium phosphate buffer (pH 6.4).

Melting temperature

Thermostability of BlaC variants was determined with the use of the hydrophobic SYPRO orange dye or using tryptophan fluorescence changes. The commercially available stock of SYPRO orange dye has a x5000 concentration, x4 concentration was used in the measurements. Tryptophan fluorescence was followed using NanoTemper Tycho NT.6 at 330 nm and 350 nm and the ratio 330 nm/350 nm was used to evaluate the melting temperature. All measurements were done in triplicates in 100 mM sodium phosphate buffer (pH 6.4).

Kinetics

All kinetic experiments were performed with the use of a PerkinElmer Lambda 800 UV-vis spectrometer at 25 °C in 100 mM sodium phosphate buffer (pH 6.4). For nitrocefin kinetics 5 nM of enzyme was used with 0 µM, 10 µM, 25 µM, 50 µM, 100 µM, 200 µM, 300 µM, and 400 µM of nitrocefin. The reactions were followed at 486 nm for 90 seconds in triplicate (extinction). The initial velocities were fit to the Michaelis-Menten equation. To measure the hydrolysis of ceftazidime, 50 nM of BlaC was used with 0 µM, 10 µM, 20 µM, 50 µM, and 100 µM ceftazidime. Product formation was measured at 260 nm for 10 minutes ($\Delta\varepsilon_{260}$ = 8 099 M^{-1} cm^{-1}). Extinction coefficient was determined with series of dilutions. Experiments were done in duplicate. Due to K_M ceftazidime being much larger than concentrations of ceftazidime used for wild type BlaC and BlaC D179N, k_{cat}/K_M value for these variants was calculated via the slope of the υ_0/[S] dependency. Errors presented in the text represent propagated standard deviations.

Inhibition assay

To measure the BlaC inhibition by avibactam, 2.5 nM of BlaC was used with 100 µM of nitrocefin in the presence of increasing amounts of avibactam, 0 µM, 10 µM, 100 µM, 500 µM. The reactions were followed at 486 nm for 20 minutes in duplicate.

NMR Spectroscopy experiments

^{15}N enriched (98%) proteins were produced as described in chapter 2 of this work. TROSY-HSQC spectra were recorded on a Bruker AVIII HD 850 MHz spectrometer at 25 °C in 100 mM phosphate buffer (pH 6.4) with 6% D2O. Data were processed in Topspin 3.2 (Bruker). Spectra were analysed with CCPNmr Analysis software V3. Peaks of the mutant spectra were assigned by comparison to peaks in the wild type BlaC spectrum and average chemical shift perturbations (CSP), Δδ, of the 1H (Δω1) and 15N (Δω2) resonances of backbone amides were calculated using equation 5.1. Peaks that could not be assigned with certainty were assigned based on the smallest possible CSP.

$$\Delta\delta = \sqrt{\frac{1}{2}\left(\Delta\omega_1^2 + \left(\frac{\Delta\omega_2}{5}\right)^2\right)} \qquad (5.1)$$

Crystallization

Crystallization conditions for BlaC D179N at a concentration of 10 mg mL^{-1} were screened for by the sitting-drop method using the JCSG+, BCS and Morpheus (Molecular Dimensions) screens at 20°C with 200 nL drops with 1:1 protein to screening condition ratio[224]. The growth appeared within four days in 0.1 M ammonium acetate, 0.1 M BIS-TRIS buffer (pH 5.5) with 0.1 M ammonium acetate and 17% w/v PEG 10K. After one month the crystals were mounted on cryoloops in mother liquor and vitrified by plunging in liquid nitrogen.

X-ray data collection, processing and structure solving

Diffraction data were collected at the Diamond Light Source (DLS, Oxford, England). The data were integrated using XDS[226] and scaled using Aimless[227] and data to 1.7 Å resolution were kept for structure solution and refinement. The structure was solved by molecular

replacement using MOLREP[228] from the CCP4 suite[228] using PDB entry 2GDN[101] as a search model. Subsequently, building and refinement were performed using Coot and REFMAC[228]. Waters were added in REFMAC during refinement; a double conformation was modelled for residue Asn110. The final model falls on the 99th percentile of MolProbity[229] and showed that 97.72% of all residues were within the Ramachandran plot favoured regions with two outliers, Cys69 and Arg220. The model was further optimized using the PDB-REDO webserver[230,231]. Data collection and refinement statistics can be found in Table 5.4.

Table 5.4. Data collection and refinement statistics for BlaC D179N.

Data Collection	D179N
Wavelength (Å)	0.912
Resolution (Å)	38.34-1.69 (1.73-1.69)
Space group	P 1 21 1
Unit cell a, b, c (Å)	38.37, 54.05, 53.64
α, β, γ	90.0, 93.2, 90.0
$CC_{1/2}$	98.8 (29.2)
R_{pim} (%)	9.7 (53.7)
|I/σI|	9.1 (1.5)
Completeness (%)	98.1 (95.9)
Multiplicity	1.8
Unique reflections	23953
Refinement	
Atoms protein/water	1988/169
B-factors protein/water (Å^2)	21/27
R_{work}/R_{free} (%)	19.8/22.3
Bond lengths RMSZ/RMSD (Å)	0.742/0.0189
Bond angles RMSZ/RMSD (°)	0.791/1.90
Ramachandran plot preferred/outliers	251/2
Ramachandran plot Z-score	-0.39
Clash score	5.07
MolProbity score	1.56

Supplementary materials

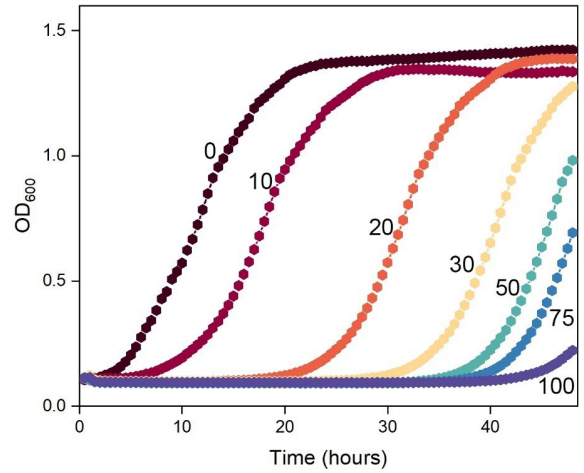

Figure S5.1. An example of the growth curves of wild type BlaC grown at 25 °C with various concentrations of ampicillin. Ampicillin concentrations presented next to the curves are in μg mL^{-1}. The duration of the horizontal phase increases upon increasing concentration of the antibiotic.

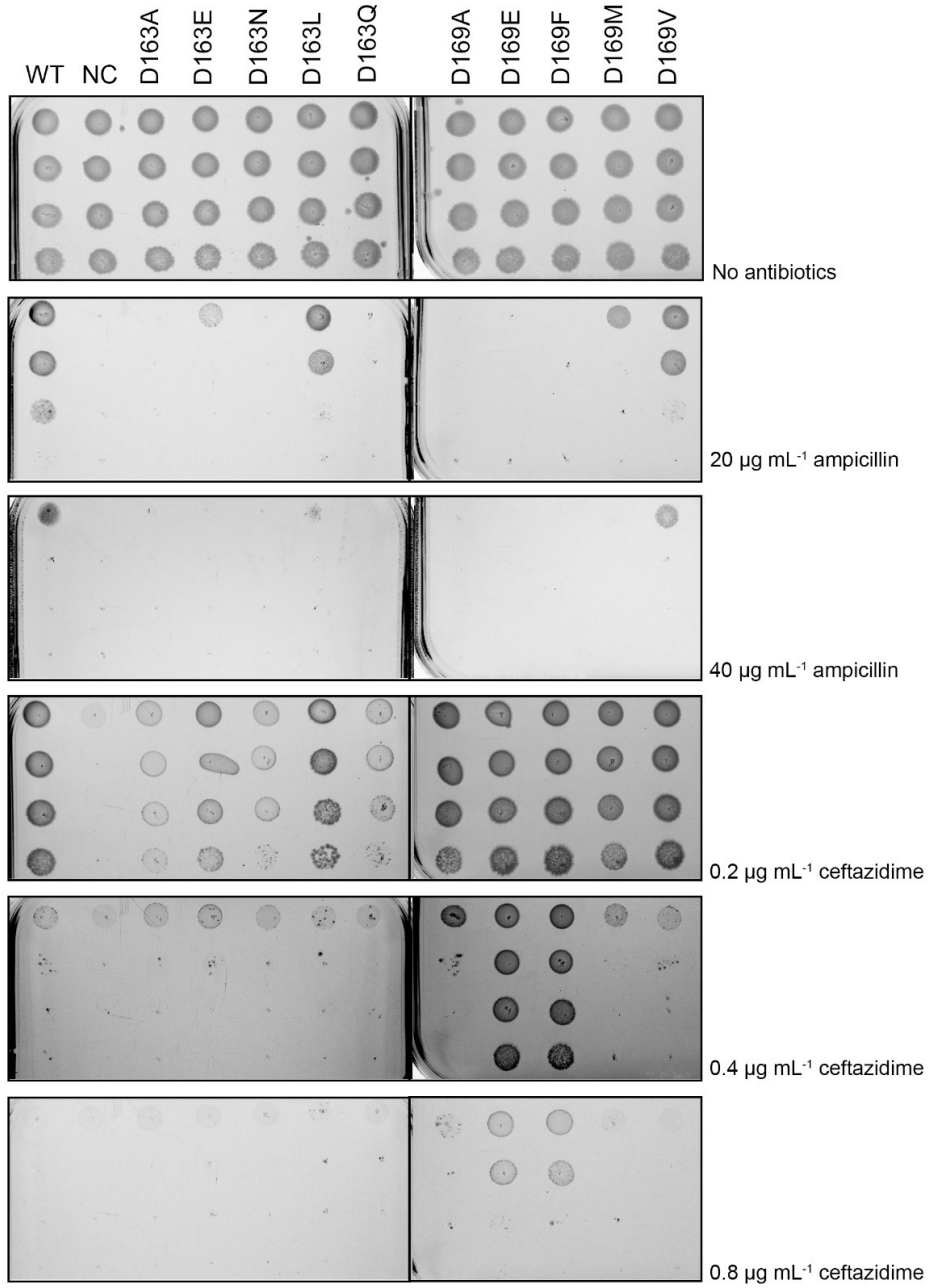

Figure S5.2. Plates showing growth of wild type BlaC and Asp163 and Leu169 variants with ampicillin and ceftazidime.

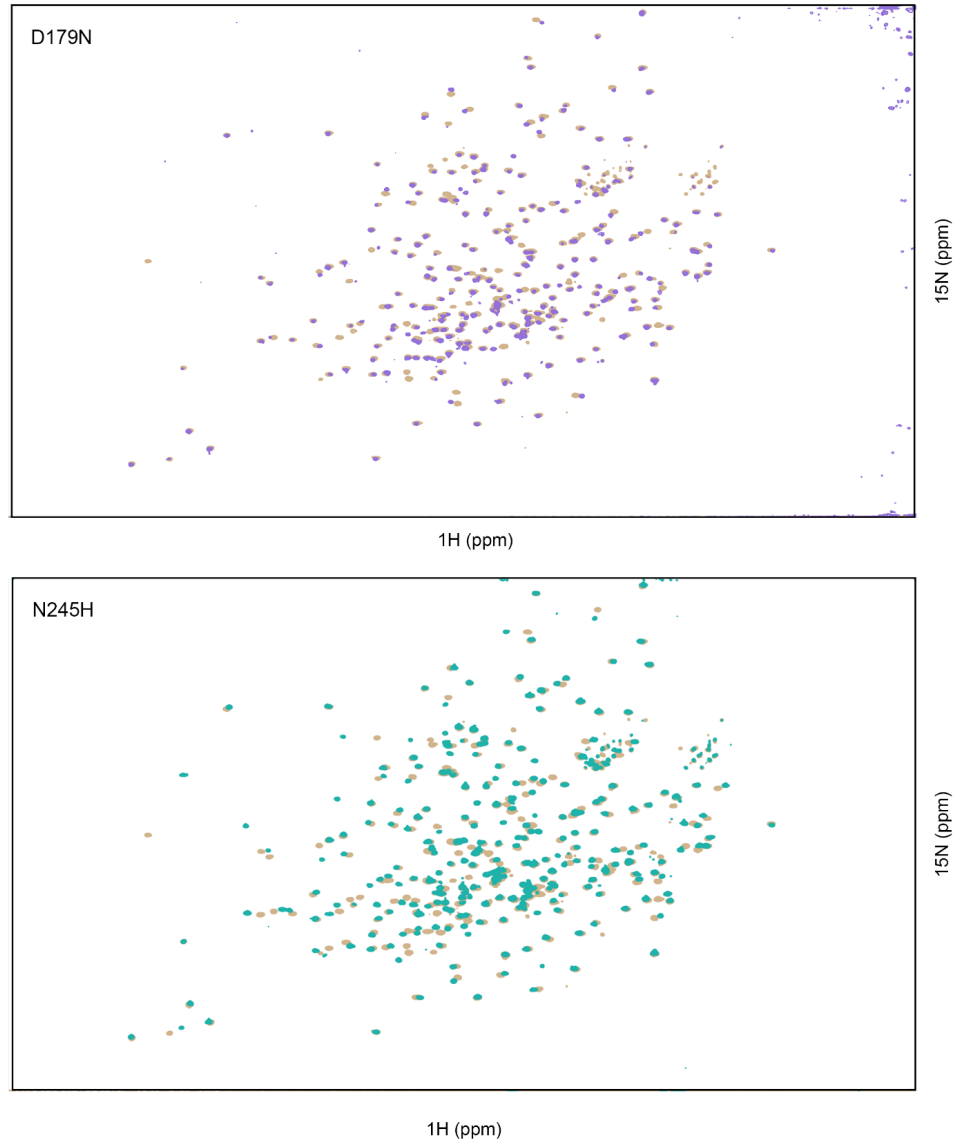

Figure S5.3. ^{15}N-^{1}H TROSY-HSQC NMR spectra of BlaC D179N (in purple) and N245H (in turquoise) overlayed on the spectrum of wild type BlaC (in beige).